Appl. Phys. B 42, 67–72 (1987)

Applied Physics B Photophysics and Laser Chemistry

Tuning Ranges of KrF and ArF Excimer Laser Amplifiers and of Associated Vacuum Ultraviolet Anti-Stokes Raman Lines

H. F. Döbele, M. Hörl, and M. Röwekamp

Fachbereich Physik, Universität-GH, D-4300 Essen 1, Fed. Rep. Germany

Received 11 August 1986/4 November 1986

Abstract. Measurements of tuning ranges for narrow-bandwidth ($\Delta\tilde{\nu} \approx 0.3\ \mathrm{cm}^{-1}$) radiation amplified in KrF and ArF laser amplifiers are reported. Generation of high-order anti-Stokes Raman lines in H_2 down to 116 nm is described as well as measurements of the corresponding tuning ranges. Generation of rotational side-bands opens the possibility to tune most of the vacuum-ultraviolet (vuv) lines over intervals in excess of $1400\ \mathrm{cm}^{-1}$. Absolute values of the power measured for the various vuv lines are communicated.

PACS: 42.65, C, 42.60.B

Discharge-pumped noble gas halide lasers represent interesting sources for the initiation of nonlinear optical processes because of their high output power. The beam quality, often unsatisfactory with standard single stage lasers, can be considerably improved by unstable resonators or – especially in the case of the ArF laser – by oscillator-amplifier combinations. This allows the application of such lasers to the generation of short wavelength radiation by stimulated Raman scattering (SRS). If the power density is sufficient, very high-order anti-Stokes (AS) Raman lines can be generated. The basic theoretical concepts are given in several articles [1–3].

Especially short wavelengths down to the far vuv can be generated in H_2 as the nonlinear medium [4]. The favourable Raman cross-section [5] together with the large Raman shift per step of $4155.247\ \mathrm{cm}^{-1}$ [6] and the weak dependence of the refractive index on wavelength [7] as well as good transmission down to 110.8 nm [8] are responsible for this advantageous behaviour.

The ArF and KrF noble-gas halide laser media are of special interest in this context since the wavelength of the emission of KrF at 248 nm and ArF at 193 nm is already close to the vuv. In addition, the transition schemes of these molecules indicate a fluorescence band broad enough to allow tuning of the laser wavelength in a spectral range of a few manometers.

Tunable vuv radiation is of interest in many fields of research. Besides applications in atomic and molecular physics, there is a demand for this kind of radiation for diagnostics in connection with fusion experiments, where laser-induced fluorescence spectroscopy (LIFS) is a well introduced diagnostic tool for the measurement of concentrations and fluxes of impurities released by sputtering from the wall of the plasma-containing vessel. This method has reached a high standard for metallic impurities in connection with dye lasers and frequency-doubling [9]. The study of the behaviour of low-Z materials, however, requires vuv radiation tuned to the wavelengths of the respective resonance lines of the impurities. For laser-pulse durations on the nanosecond time scale, the power has to be in the kilowatt range [10]. For this application, the spectral intervals around 166 and 156 nm are of special interest because of the resonance lines of carbon, beryllium, boron and silicon. The resonance triplet of oxygen, a species of central importance as a plasma impurity, is located close to 130 nm.

Spectral tuning of ArF and KrF lasers has been reported by several authors (see, e.g., [11]). With prism-grating combinations, tuning is possible over a considerable fraction of the width of the fluorescence band. The spectral width of the laser radiation that can be obtained by this method is of the order of $10\ \mathrm{cm}^{-1}$. If, on the other hand, a narrow line-width well below

$1\ cm^{-1}$ is required, this can be obtained by using additional dispersive elements in the laser cavity, e.g. intracavity etalons, with the consequence that the tuning range is considerably reduced to approximately 1 nm in the case of ArF [12]. Assuming such a tuning range for narrow-bandwidth operation of an ArF laser as an upper limit to the respective anti-Stokes lines, it becomes obvious that some but not all of the important transitions can be excited.

In several contributions amplification in noble-gas halide lasers has been reported where the radiation to be amplified is not supplied by an oscillator working with the same medium but is generated from dye laser radiation in connection with methods of nonlinear optics [13, 14]. This allows to feed the amplifier with narrow-bandwidth radiation of constant input power even in the wings of the fluorescence line of the amplifier medium and to obtain amplification over a considerably larger spectral interval than with a conventional oscillator-amplifier combination.

In this paper we report on amplification in KrF and ArF laser amplifiers and on Raman conversion of the laser frequency up to vuv wavelengths well below L_α. We communicate the tuning ranges and the power obtained at the various anti-Stokes Raman lines.

Experimental

In the present study, the generation of the laser radiation to be amplified in ArF and KrF starts with a XeCl-laser-pumped dye laser (Lambda Physik EMG 200 E/FL 2002). The radiation to be amplified in KrF around 248 nm is generated by two methods: Frequency doubling (SHG) of dye laser radiation (dye Coumarin 307) in a potassium pentaborate (KPB) crystal, or, alternatively, by stimulated Raman scattering in H_2. In the latter case radiation around 248 nm is generated in three anti-Stokes steps starting with dye laser radiation (dye DMQ) at 360 nm. The Raman cell is of the same kind as the one described below in connection with vuv generation. In both cases we obtained approximately 0.2 mJ at 248 nm. Both methods require comparable expenses: for SHG in this wavelength range a KPB crystal is necessary which is relatively sensitive to damage. A computer-controlled tuning unit is required to synchronize the stepping motors of the dye laser grating and of the SHG crystal. For the Raman conversion, on the other hand, a hydrogen cell (preferably surrounded with a well insulated container for liquid nitrogen) has to be provided. In the latter case, the output radiation contains all Raman-orders simultaneously.

For amplification in ArF at 193 nm the primary radiation is generated only by Raman conversion (6^{th} AS line) of dye-laser radiation at 372 nm (dye QUI: up to 30 mJ). Up to 60 μJ are obtained under optimum conditions. For these experiments all optical elements following the first hydrogen cell are located in a nitrogen atmosphere to avoid absorption by oxygen. After amplification in two ArF-laser sections (Lambda Physik EMG 100 E + EMG 200 E) the energy amounts to approximately 100 mJ. With optimum performance of all units including the dye laser, up to 150 mJ are possible. This is also the maximum value we measured for the amplification in KrF at 248 nm. A mask adapted to the shape of the amplified pattern is installed on the exit side of the second amplifier stage. Its purpose is to screen amplified spontaneous radiation generated in the excimer sections. The operation parameters of the excimer sections correspond to the recommendations of the manufacturer: (ArF: F_2 – 7.5 mbar, Ar – 350 mbar, He – 1440 mbar/KrF: F_2 – 6 mbar, Kr – 120 mbar, He – 2370 mbar).

Figure 1 shows the laser system with the hydrogen cells and the components for the dispersion and power measurements of the vuv radiation.

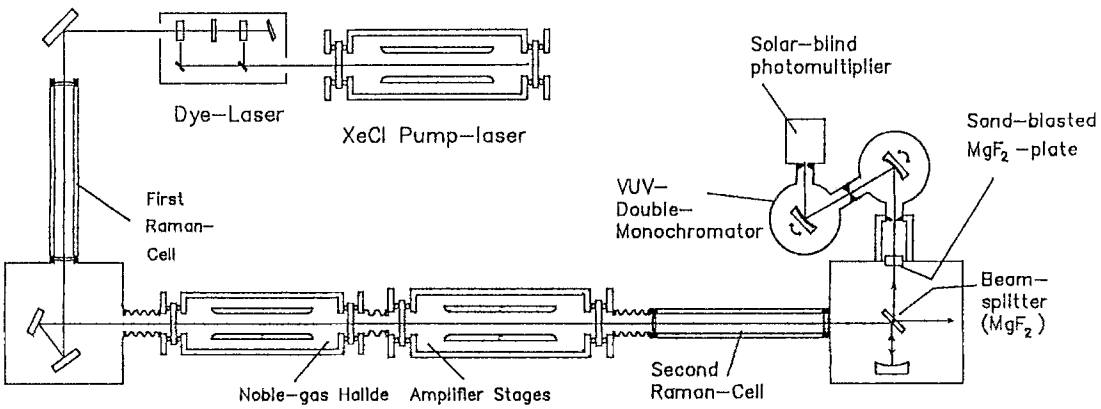

Fig. 1. Experimental set-up for generation of vuv radiation and power measurements. The version is shown with generation of vuv radiation by SRS before amplification. Details are explained in the text

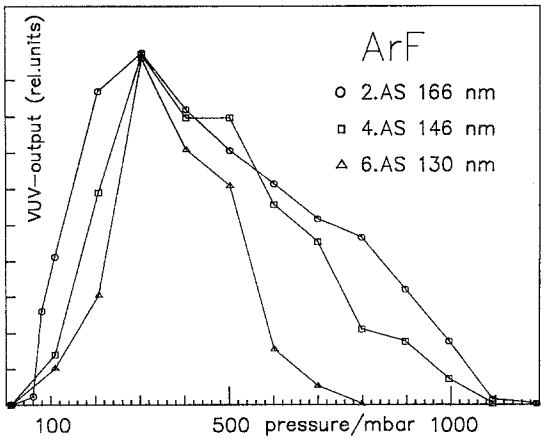

Fig. 2. Pressure dependence of vuv power of different AS lines generated in liquid nitrogen cooled hydrogen

The three excimer stages are driven from a main trigger unit. The switching times of the two amplifiers and the XeCl pump laser can be shifted by a variable time-delay. The correct setting of the delay is achieved by observing simultaneously the light pulse generated in the first Raman cell and the fluorescence radiation of the amplifier stages and adjusting the time delay until the amplified signal is optimized. This optimum operation is recognized easily since the length of the amplified pulse is considerably shorter (≈ 5 ns) than the one of the fluorescence (≈ 15 ns). The quality of the synchronization of the excimer discharges is continuously monitored by observing with a photodiode the weak fluorescence coming off the lateral circumference of the entrance lens of the second hydrogen cell. With 3-Hz-operation corrections to the delay settings are necessary after typically one hour.

The amplified radiation is focussed by an $f = 60$ cm MgF_2 lens, acting simultaneously as window, into the second Raman cell. This cell consists of a stainless steel tube, 120 cm long and 4 cm in diameter. Its central part is surrounded by an 80 cm long thermally insulated tin housing, filled with liquid nitrogen. The cooling is intended to freeze-out contaminations, mainly H_2O, and to give some additional increase in Raman conversion by narrowing the Raman line width [15]. The optimum pressure in the case of cooling with LN_2 is in the range of 300 mbar as can be seen from Fig. 2 which shows the pressure dependence of some of the AS lines. For all measurements described below, the pressure was kept in this range. An MgF_2 flat serves as exit window of the cell.

The output radiation can be attenuated by a set of meshes with different transmission factors. These wavelength-independent filters are mounted in a vacuum chamber on a disc and the appropriate attenuation can be selected by means of a feed-through for disc rotation. The radiation is then partially reflected off the surface of an MgF_2 plate oriented at 45 degrees (Fig. 1) and is focussed by an aluminized concave mirror. A frosted MgF_2 plate is located close to this focal position and illuminates the entrance slit of a vacuum double-monochromator (two Minuteman $f = 200$ mm in series with a common intermediate slit). This relatively complicated optical scheme was chosen in order to provide uniform illumination of the monochromator despite the various AS orders leaving the Raman cell with different conus angles. A solar-blind photomultiplier (EMI Gencom G 26 H 315) was used to measure the intensities. Its signal – together with the signal of the photodiode monitoring the amplifier radiation at the entrance window as mentioned above – is digitized and stored in a computer. This computer starts the main trigger of the excimer lasers and also controls the stepping motors of the two monochromator gratings as well as that of the dye laser.

Measurements

Figure 3 shows the intensities of the laser radiation amplified in KrF and ArF as function of the wavelength of the primary radiation. The corresponding measurements for some of the anti-Stokes lines are shown in Fig. 4. The spectral intervals in which Raman-shifted radiation can be generated turn out to be only slightly narrower than the tuning range of the primary laser sources. Figure 5 gives the tuning ranges of the anti-Stokes orders generated with laser radiation amplified in ArF. In the measurements of these tuning ranges, only those signals were considered which correspond to pump-pulse energies within $\pm 50\%$ of the average energy. Each point in the recording of these tuning ranges is an average of 20–40 pulses. The peak occurring within the tuning range of the 117 nm AS line is caused by stimulated emission in the Werner

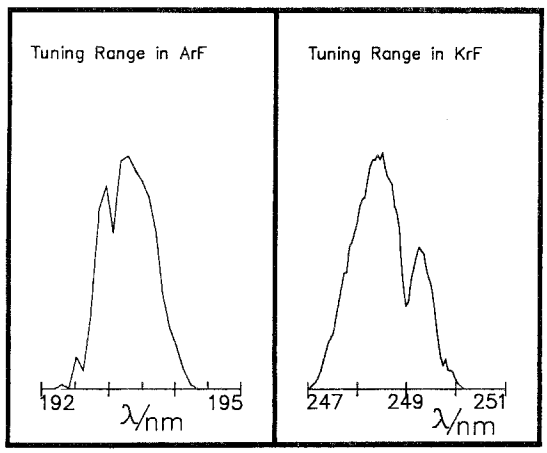

Fig. 3. Tuning ranges of laser radiation amplified in KrF and ArF excimer laser amplifiers

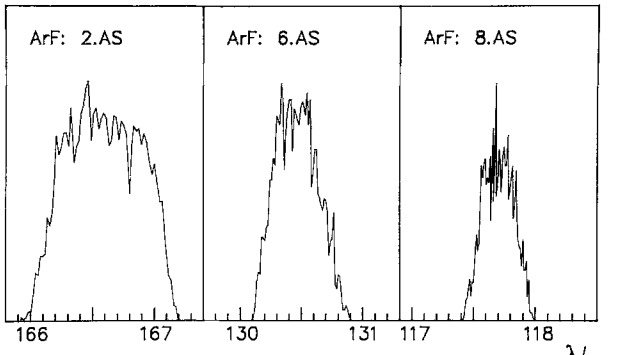

Fig. 4. Tuning ranges of some anti-Stokes lines

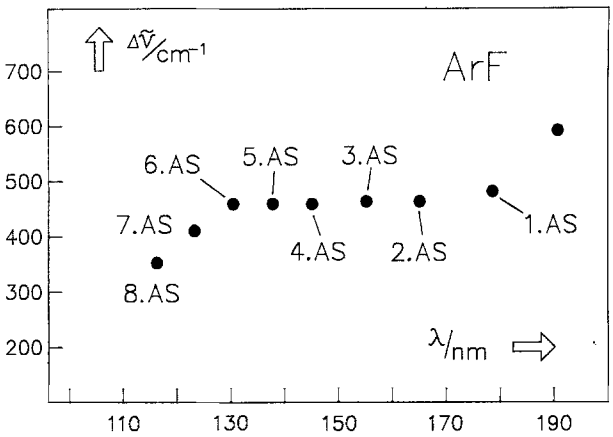

Fig. 5. Tuning ranges of anti-Stokes lines of laser radiation amplified in ArF laser amplifiers

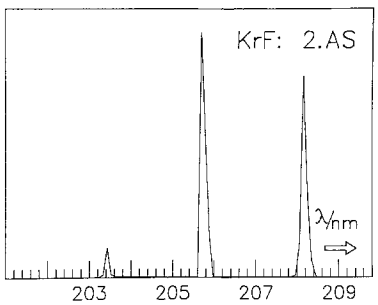

Fig. 6. Vibrational transition at 206 nm and rotational satellites of the 2nd anti-Stokes component generated by 248 nm radiation. The primary radiation at 248 nm is generated by Raman-conversion in H_2 and amplified in KrF laser amplifiers

band following two-photon excitation of hydrogen into the $E, F^1\,\Sigma_g^+$ – electronic configuration. This effect is discussed in a separate publication [16].

The energy in the various AS lines, as shown in Fig. 4 corresponds to the pure vibrational transition which is generated with linearly polarized radiation. The pulse durations are 3–4 ns for the lines generated with 193 nm radiation and 4–5 ns in the other case. If the pump radiation is elliptically polarized (this can be accomplished, e.g., by inserting a slightly tilted MgF_2 plate in front of the Raman cell) we observe additional rotational

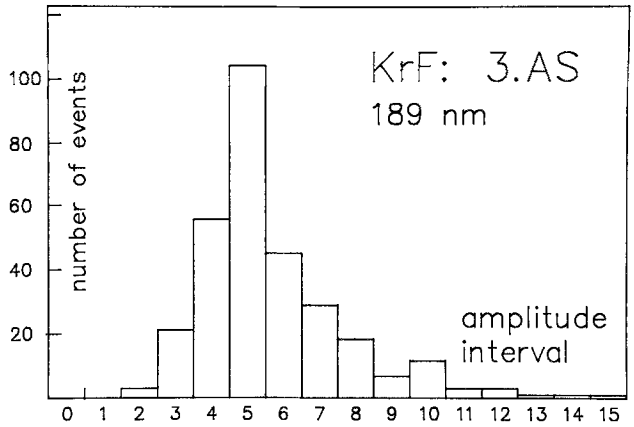

Fig. 7. Probability distribution of the amplitude of 315 anti-Stokes pulses

transitions separated by 587 cm^{-1} [6]. These correspond to the $S(1)$ (red satellite) and the associated AS transition. The red side-line is of comparable or even higher intensity than the vibrational transition whereas the blue line is considerably weaker. In case of the first AS line at 225 nm (generated with 248 nm radiation), we observe, in addition, higher-order (up to 5) rotational side-lines, equally spaced by 587 cm^{-1}. For the two highest-order vibrational AS lines (122 and 116 nm), the blue side-lines are not observed. Figure 6 shows the triplet for the second anti-Stokes component of KrF.

Especially for high anti-Stokes orders, intensity fluctuations become important. We have investigated the statistics of these fluctuations for several AS lines. Figure 7 shows the situation for the 3rd AS component at 189 nm, generated with laser radiation amplified in KrF around 248 nm. For these measurements, only pump pulses at 248 nm have been included with an energy within the $\pm 10\%$ range of the mean value. The determination of absolute intensities of the vuv Raman components represents a considerable problem because the range of intensities covers several orders of magnitude. In an earlier investigation [14] the relative spectral sensitivity of the monochromator together with the solar blind photomultiplier was determined with the aid of a deuterium calibration lamp. In this work, we apply an argon arc source developed at NBS [17]. The continuous vuv spectrum of this "argon mini-arc" is used for calibration. For this measurement, the mini-arc was located at the position of the focus in the second hydrogen cell with all the optical components including the frosted MgF_2 disc in their original positions. In order to measure the low intensity, it was necessary to chop the radiation and to apply lock-in detection. The relative spectral sensitivity obtained in this way was related to an absolute scale by recording the first two AS lines generated with radi-

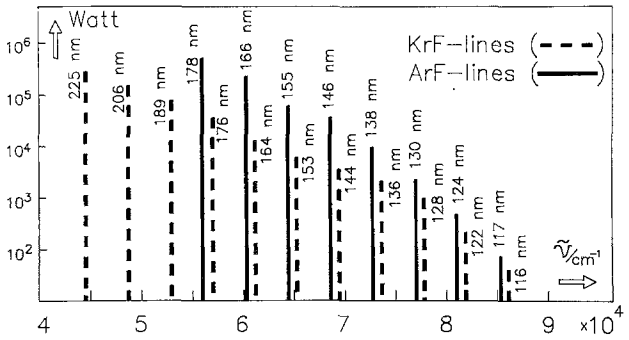

Fig. 8. Pulse-power of the various AS lines generated by radiation amplified in KrF and ArF amplifiers

ation amplified in KrF with this monochromator-photomultiplier combination and by measuring their energies independently with a laser energy meter (Gentec type ED 200) after spectral dipersion with a quartz prism. This calibration yields, together with a separate measurement of the transmission factors of the meshes used for attenuation, the power shown in Fig. 8 of the various AS lines. The values given refer to the center of the corresponding tuning ranges. The values are in satisfactory agreement with earlier measurements [14] where a deuterium lamp was used. In view of the various factors influencing these vuv power measurements, we consider the reported values reliable within a factor of two or three.

Conclusions

The amplification of laser radiation generated by stimulated Raman scattering (amplification in ArF and KrF) or by SHG (amplification in KrF) in excimer-laser amplifiers results in a considerably larger tuning range compared to tunable ArF or KrF laser systems, in particular if narrow-linewidths (of the order of some tenths of a wave number) are important. Focussing of the amplified radiation in a hydrogen-filled Raman cell results in simultaneously generated anti-Stokes and Stokes components of many orders. The vuv radiation leaves the cell in a conical shape with different angles for different Raman orders [18].

The investigation of the spectral intervals in which amplification occurs for KrF and ArF laser media yields values of 505 and 590 cm^{-1}, respectively. The corresponding AS components are generated within a spectral interval of 440 cm^{-1} for excitation with radiation amplified in KrF and 490 cm^{-1} for excitation with radiation amplified in ArF except for the highest anti-Stokes orders where the intervals are somewhat smaller.

In case of the highest AS order generated with ArF radiation occurring at 117 nm, we find an intense peak which is explained as a two-photon excitation into the $E, F^1\Sigma_g^+$-configuration followed by a subsequent transition to a neighbouring level of the $C^1\Pi_u$-configuration [19] which decays by stimulated emission to the $v=5$ vibrational level of the $X^1\Sigma_g^+$-configuration of H_2. In addition to this line, a number of transitions (23 lines) in the Werner and Lyman bands were observed. Further details are communicated in another publication [16].

The occurrence of rotational side-lines at a spectral distance of 587 cm^{-1} opens the possibility to tune the vuv lines continuously over a spectral interval in excess of 1400 cm^{-1} since the tuning range of the central component exceeds half the spectral distance to the rotational side-lines.

The reproducibility of the intensity obtained in high anti-Stokes orders can be summarized as follows: For the AS lines with wavelengths around 150 nm or longer, about 50% of the pulse energies are within $\pm 20\%$ of the mean value. In the case of the transition shown in Fig. 7, the situation is even better. For the high orders, on the other hand, one can assume that 50% of the pulses are within $\pm 50\%$ of the mean energy.

This behaviour may be unsatisfactory for some applications. However, present-day excimer-laser systems allow repetition rates in excess of ten or even some 100 Hz. It is therefore possible without inacceptable increase of measuring time to set limits for the vuv pulse-powers and to consider only those events with vuv energies within the specified range. For the application to fluorescence diagnostics of plasmas, one has to distinguish situations where the saturation parameter [20] is much smaller or much larger than one. In the first case it is possible to monitor the vuv pump signal together with the fluorescence signal and to normalize the latter, whereas in the second case the fluorescence signal is largely independent of the pump intensity, so that fluctuations can be tolerated.

The measurements described in this paper show that stimulated Raman scattering of dye-laser radiation and of radiation amplified in excimer sections represents a powerful and convenient source for tunable vuv radiation. If the necessary wavelengths are located in the long-wavelength part of the vuv, between 200 and 150 nm, and if moderate power in the range of hundred watts to one kilowatt is sufficient, the optimum choice is SRS with a dye laser [21]. If, on the other hand, high power especially at shorter wavelengths is required, amplification in excimer sections is necessary. In this case the tuning range is related to the width of the fluorescence band of the excimers, although the occurrence of rotational side-lines leads to tuning ranges of approximately 1400 cm^{-1} except for the highest orders. From comparable observations in the visible and near uv of the occurrence of

rotational components on both sides of the vibrational transition [22], we conclude that it is very likely that with suitably chosen polarization of the pump radiation even higher order rotational side-lines may be generated. Thus in case of the vuv-AS lines a further increase of the tuning ranges appears to be feasible.

Raman-converted vuv radiation has been applied meanwhile to several fluorescence experiments. Atomic oxygen generated in a flow-tube system was excited and detected with 130 nm radiation [23] as well as beryllium (which is presently discussed as a candidate for fusion-machine walls) which was evaporated in a Knudsen cell [24]. In another experiment, the velocity distribution of carbon atoms sputtered off carbon and TiC targets by impinging argon ions has been determined by application of narrow-bandwidth radiation at 166 nm using the Doppler effect. The pump radiation with a line-width of $\Delta\tilde{\nu} \approx 0.1\ \mathrm{cm}^{-1}$ was continuously tuned and the integral fluorescence radiation was detected by a solar-blind photomultiplier [25].

These first applications of Raman-converted vuv radiation show that this vuv source opens new and interesting possibilities for fluorescence diagnostics of atoms and molecules.

Acknowledgements. Helpful discussions with Dr. B. Rückle of Lambda Physik, Göttingen and Dr. B. Reimann of the Max-Planck-Institut für Strahlenchemie, Mülheim, are gratefully acknowledged. We thank J. Leistikow for skillful technical assistance. This work was supported by the Deutsche Forschungsgemeinschaft.

References

1. A. Penzkofer, A. Lauberau, W. Kaiser: Progr. Quantum Electron. **6**, 55–140 (1979)
2. D.C. Hanna, M.A. Yuratich, D. Cotter: *Nonlinear Optics of Free Atoms and Molecules*, Springer Ser. Opt. Sci. **17** (Springer, Berlin, Heidelberg 1979)
3. Y.R. Shen: *The Principles of Nonlinear Optics* (Wiley, New York 1984)
4. R.S. Hargrove, J.A. Paisner: "Tunable, efficient vuv generation using ArF-pumped, stimulated Raman scattering in H_2", in Dig. Top. Meeting Excimer Lasers, Opt. Soc. Am., Washington, DC (1979) paper ThA6
5. H.W. Schrötter, H.W. Klöckner: "Raman Scattering Cross-Sections in Gases and Liquids", in *Raman Spectroscopy*, ed. by A. Weber, Topic Cur. Phys. **11** (Springer, Berlin, Heidelberg 1979) pp. 123–197
6. S.L. Bragg, J.W. Brault, W.H. Smith: Astrophys. J. **263**, 999 (1982)
7. Landolt-Börnstein: *Zahlenwerte und Funktionen*, Vol. 2, Part 8, 6–885 (Springer, Berlin, Heidelberg 1962) 6th ed.
8. H. Okabe: *Photochemistry of Small Molecules* (Wiley, New York 1978)
9. P. Bogen, B. Schweer, H. Ringler, W. Ott: J. Nucl. Mater. **111 &112**, 67 (1982)
10. H.F. Döbele, M. Röwekamp, B. Rückle: J. Nucl. Mater. **128 &129**, 986 (1984)
11. T.R. Loree, K.B. Butterfield, D.L. Baker: Appl. Phys. Lett. **32**, 171 (1978)
12. B. Rückle et al.: Conference on Lasers and Electro-Optics (CLEO), San Francisco (1986)
13. J.C. White, J. Bokor, R.R. Freeman, D. Henderson: Opt. Lett. **6**, 293 (1981)
14. H.F. Döbele, M. Röwekamp, B. Rückle: IEEE J. QE-**20**, 1284 (1984)
15. D.J. Brink, D. Proch: Opt. Lett. **10**, 494 (1982)
16. H.F. Döbele, M. Hörl, M. Röwekamp: Appl. Phys. Lett. **49**, 925 (1986)
17. J.M. Bridges, W.R. Ott: Appl. Opt. **16**, 367 (1976)
18. D.J. Brink, D. Proch: J. Opt. Soc. Am. **73**, 23 (1983)
19. H. Pummer, H. Egger, T.S. Luk, T. Srinivasan, C.K. Rhodes: Phys. Rev. A **28**, 795 (1983)
20. P. Bogen, E. Hintz: Comments Plasma Phys. Cont. Fusion **4**, 115 (1978)
21. H. Schomburg, H.F. Döbele, B. Rückle: Appl. Phys. B**30**, 131 (1983)
22. V. Wilke: Erzeugung frequenzvariabler Strahlung durch stimulierte Ramanstreuung an Wasserstoff. Thesis, Universität-GH Essen (1979)
23. H.F. Döbele, M. Hörl, M. Röwekamp, B. Reimann: Appl. Phys. B**39**, 91 (1986)
24. U. Czarnetzki, H.F. Döbele, M. Hörl, M. Röwekamp, B. Reimann, V. Schulz-von der Gathen: J. Nucl. Mater. **145&146** (1986) (to appear)
25. P. Bogen, H.F. Döbele, Ph. Mertens: J. Nucl. Mater. **145&146** (1986) (to appear)